NASA Technical Paper 3072

April 1991

A Controls Engineering Approach for Analyzing Airplane Input-Output Characteristics

P. Douglas Arbuckle

NASA

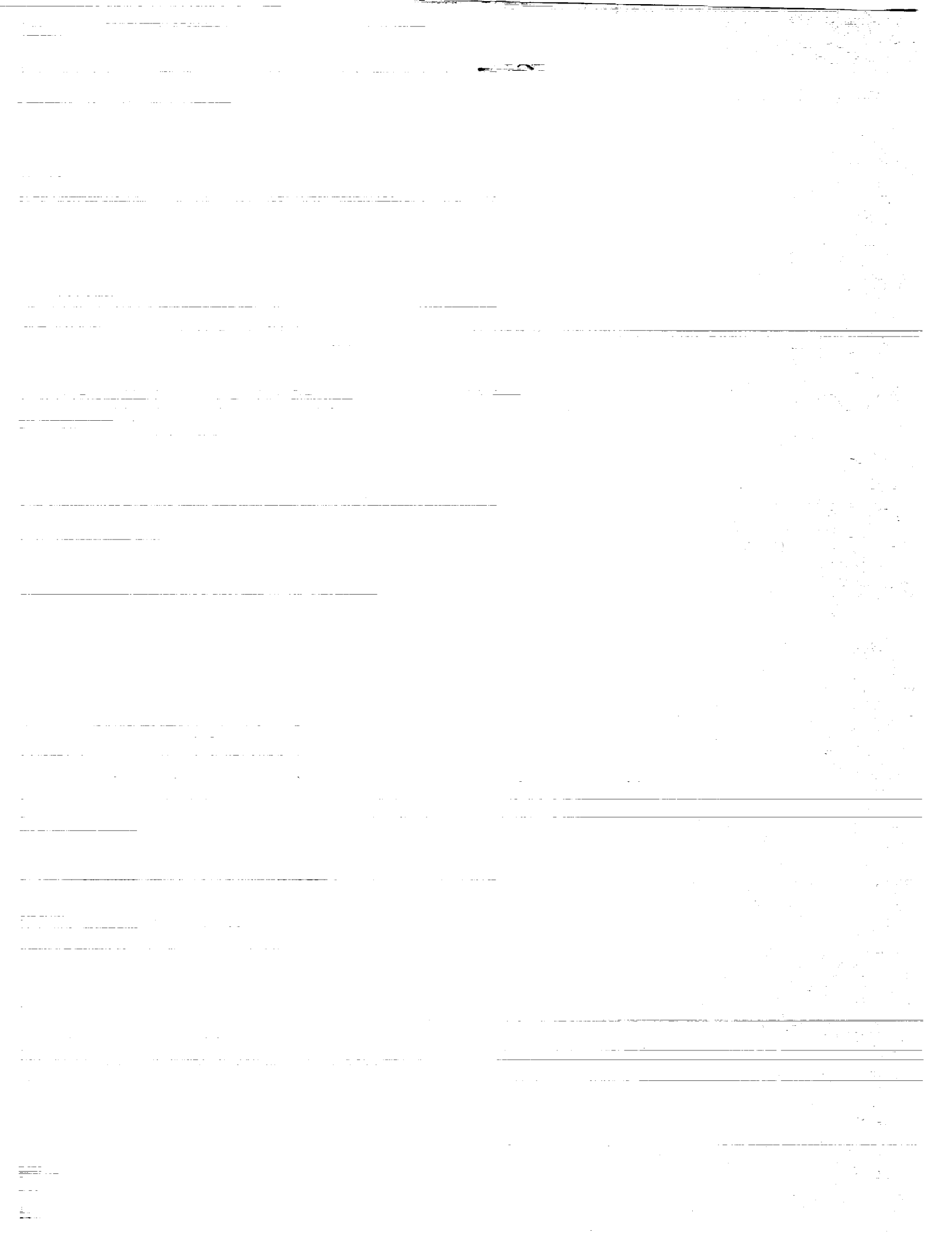

NASA Technical Paper 3072

1991

A Controls Engineering Approach for Analyzing Airplane Input-Output Characteristics

P. Douglas Arbuckle
Langley Research Center
Hampton, Virginia

NASA
National Aeronautics and Space Administration
Office of Management
Scientific and Technical Information Division

Nomenclature

$\mathbf{A}$	system dynamics matrix ($n \times n$)
$\mathbf{B}$	input distribution matrix ($n \times m$)
$\mathbf{C}$	state-to-output distribution matrix ($l \times n$)
$\mathbf{C}_e$	relative modal control effectiveness matrix ($n' \times m$)
$\mathbf{c}$	unit-length steady-state input perturbation m-vector
$c_{e_{\ell,j}}$	normalized relative modal control factor, or element of $\mathbf{C}_e$ ($\ell = 1$ to n', $j = 1$ to m)
$\mathbf{D}$	input-to-output distribution matrix ($l \times m$)
i	imaginary number, $\sqrt{-1}$
J	objective function
l	number of output perturbation quantities
m	number of input perturbation variables
n	number of state perturbation variables
n'	number of system modes
$\mathbf{O}$	relative output significance matrix ($l \times n'$)
$o_{k,\ell}$	normalized relative modal observability factor, or element of $\mathbf{O}$ ($k = 1$ to l, $\ell = 1$ to n')
p	roll rate perturbation in airplane body axis, deg/sec
$\mathbf{Q}$	steady-state input-to-output distribution matrix ($l \times m$)
$\mathbf{q}_k$	m-vector formed by the kth row of $\mathbf{Q}$
q	pitch rate perturbation in airplane body axis, deg/sec
r	yaw rate perturbation in airplane body axis, deg/sec
$\mathbf{S}$	optimization matrix ($m \times m$)
t	time, sec
$\mathbf{u}$	input or input perturbation m-vector
u_j	input perturbation variable ($j = 1$ to m)
$\mathbf{V}$	nonsingular transformation matrix between scaled and modal coordinates ($n \times n$)
V_t	airplane total velocity perturbation, ft/sec
$\mathbf{W}$	diagonal weighting matrix used for scaling
$\mathbf{x}$	state perturbation n-vector
x_i	state perturbation variable ($i = 1$ to n)
$\mathbf{y}$	output perturbation l-vector
y_k	output perturbation variable ($k = 1$ to l)
α	angle-of-attack perturbation, deg
β	angle-of-sideslip perturbation, deg
$\mathbf{\Gamma}$	modal controllability matrix ($n \times m$)
$\gamma_{i,j}$	element of $\mathbf{\Gamma}$ ($i = 1$ to n, $j = 1$ to m)
δ	perturbation of control surface, throttle lever, or thrust vector, deg
θ	Euler pitch angle perturbation, deg
$\mathbf{\Lambda}$	modal dynamics matrix, block diagonal ($n \times n$)
λ_i	eigenvalue or element of $\mathbf{\Lambda}$ ($i = 1$ to n), rad/sec
$\boldsymbol{\xi}$	state perturbation n-vector in modal coordinates
σ_i	real part of eigenvalue λ_i, rad/sec
$\mathbf{\Phi}$	modal observability matrix ($l \times n$)
$\varphi_{k,i}$	element of $\mathbf{\Phi}$ ($k = 1$ to l, $i = 1$ to n)
ϕ	Euler bank angle perturbation, deg
ψ	Euler heading angle perturbation, deg
ω_i	imaginary part of eigenvalue λ_i, rad/sec

Subscripts:

a	aileron
as	antisymmetric
f	trailing-edge flap

n	leading-edge flap
r	rudder
s	horizontal stabilator
ss	steady state
sy	symmetric
th	engine throttle lever
tv	thrust vectored

Superscripts:

s	scaled quantity
T	transpose of matrix $[\cdot]$
$*$	estimated best value for scaling
-1	inverse of matrix $[\cdot]$
$\dot{(\ )}$	derivative with respect to time, d/dt

Abbreviations:

D.R.	Dutch roll
Phug.	phugoid
S.P.	short period
Spir.	spiral

Abstract

An engineering approach for analyzing airplane control and output characteristics is presented. State-space matrix equations describing the linear perturbation dynamics are transformed from physical coordinates into scaled coordinates. The equations are scaled by applying various transformations that employ prior engineering knowledge of the airplane physics. Two analysis techniques are then explained. Modal analysis techniques calculate the influence of each system input on each fundamental mode of motion and the distribution of each mode among the system outputs. The optimal steady-state response technique computes the blending of steady-state control inputs that optimize the steady-state response of selected system outputs. An example airplane model is analyzed to demonstrate the described engineering approach.

Introduction

For the early phases of control system design and analysis, engineers typically use a model of the airplane dynamics represented by linear state-space equations. The control design cycle usually begins with an analysis of the basic airplane without automatic controls, followed by an engineering determination of the appropriate control structure and subsequent calculation of the control system gains. The engineer then analyzes and evaluates the airplane model including the control system. Depending on the results of the analysis, the engineer may choose to adjust the design until it can be "frozen" and implemented in nonlinear simulation for additional analysis. Figure 1 depicts this process.

As airplane designers attempt to extract more and more performance from each new configuration, controls engineers are increasingly confronted with airplane models that have a large number of inputs and/or outputs (possibly redundant) and higher order dynamics. Under these conditions, it becomes more difficult for the engineer to directly apply traditional analysis techniques and produce results that are readily understood.

This report presents a systematic engineering approach for analyzing linear state-space equations. Many of the relations presented are commonly used by engineers and can be obtained either directly or indirectly as by-products of the design process. For example, the engineer frequently wishes to compare the sizes of elements in particular matrices. Computing the relative sizes directly assists the engineer in envisioning and understanding the physics of a given problem. A formalized approach of scaling states, inputs, and outputs is presented to accomplish this.

Although some extensions to the literature are proposed, the primary goal of this report is not to present new theory, but to emphasize the engineering aspects of dynamics analysis for the control system designer. An example is used to illustrate the types of observations that can be made when applying these analysis techniques.

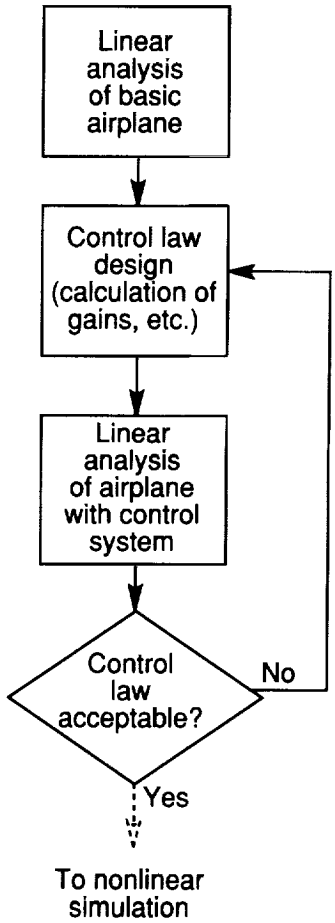

Figure 1. Linear control design and analysis process.

Mathematical Development

This section describes the mathematical development of the engineering analysis approach. In addition to a traditional presentation of theory, engineering assumptions or implementation issues are also described. A diagram showing the hierarchy of the analysis approach is shown in figure 2. Beginning with a state-space description of a linear system, the system is converted from physical coordinates to scaled coordinates. The scaled system is used as the basis for all subsequent analysis. One analysis technique transforms the scaled system to modal coordinates and then manipulates the controllability and observability matrices to compute quantities that indicate the relative effect of the inputs on the modes and the appearance of these modes in the outputs. The second analysis technique uses the scaled system to compute the "blend" of steady-state inputs that "optimize" one or more steady-state outputs.

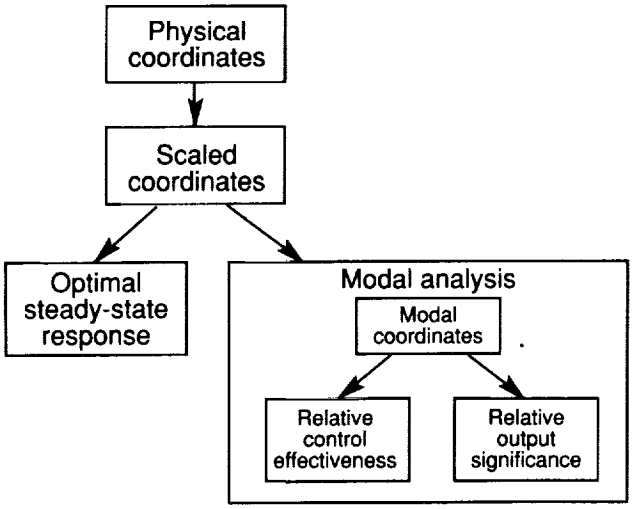

Figure 2. Hierarchy and flow diagram for engineering analysis approach.

State-Space Description of Linear Dynamic Systems

The motion of many dynamic systems can be described by a set of equations in the form

$$\left.\begin{aligned}\dot{\mathbf{x}} &= \mathbf{f}_1(\mathbf{x},\mathbf{u})\\ \mathbf{y} &= \mathbf{f}_2(\mathbf{x},\mathbf{u})\end{aligned}\right\} \tag{1}$$

where $\mathbf{x}$ is a vector of time-varying state variables, $\mathbf{u}$ is a vector of input variables, and $\mathbf{y}$ is a vector of output variables. The input variables $\mathbf{u}$ can be any combination of force or moment generators, pilot or command inputs, process noise or gust inputs, and measurement noise inputs. In the literature a separate term is commonly defined for each type of input quantity, but here and in the subsequent developments they are grouped for notational compactness.

Equations (1) can be linearized about a reference condition. This reference condition is usually an equilibrium point. The resulting linear equations, valid for small perturbations from the reference condition, are

$$\left.\begin{aligned}\dot{\mathbf{x}} &= \mathbf{A}\mathbf{x} + \mathbf{B}\mathbf{u}\\ \mathbf{y} &= \mathbf{C}\mathbf{x} + \mathbf{D}\mathbf{u}\end{aligned}\right\} \tag{2}$$

where $\mathbf{A}$ is the system dynamic matrix, $\mathbf{B}$ is the input distribution matrix, $\mathbf{C}$ is the state-to-output distribution matrix, and $\mathbf{D}$ is the input-to-output distribution matrix. Equations (2) are called the linear state-space system equations, with the variables $\mathbf{x}$, $\mathbf{u}$, and $\mathbf{y}$ being vectors of perturbation quantities. For this report, the reference condition is an equilibrium point; therefore, $\mathbf{A}$, $\mathbf{B}$, $\mathbf{C}$, and $\mathbf{D}$ are time invariant.

Scaled Coordinates

Interpretation of dynamic system behavior can be cumbersome because of the variety of units and magnitudes of the parameters used to describe dynamic motions. In a wide range of airplane problems scaling of variables can make the analysis more coherent. For example, aerodynamicists have long known the benefits of using nondimensional coefficients to analyze and compare various configurations.

Most efforts directed at solving the scaling problem consist of enforcing a common angular measure (either degrees or radians) and sometimes scaling all velocity elements by the total vehicle velocity at trim (ref. 1). This subsection presents a different technique for scaling state perturbation variables, input perturbation variables, and output perturbation variables. The purpose for this scaling concept is to provide a common basis for comparison in the analysis. As an example, this concept results in scaling of the inputs (controls) on the basis of each control effector's maximum authority (limit). This scaling concept also enables engineering knowledge of the airplane dynamics to be captured and used in the analysis.

Any system can be scaled by applying a similarity transformation to its state variable representation (ref. 2). Such a transformation does not affect the eigenvalues of a system. Therefore, to scale the state perturbation variables, define

$$\mathbf{x} = \mathbf{W}_x\mathbf{x}^s \tag{3}$$

where $\mathbf{x}^s$ is the scaled state perturbation vector and $\mathbf{W}_x$ is an $n \times n$ diagonal matrix,

$$\mathbf{W}_x \equiv \text{diag}\,(x_1^*,\ x_2^*,\ \ldots,\ x_i^*,\ \ldots,\ x_n^*) \qquad (4)$$

where x_i^* is the estimated best value for scaling state perturbation variable x_i so that, in general

$$\left|\frac{x_i}{x_i^*}\right| \leq 1.0 \qquad (5)$$

is true for all time. A good value for x_i^* in most cases would be the predicted maximum value of the state perturbation variable x_i. This predicted maximum value of the state perturbation variable should be chosen to define the region of linearity for the model. The choice of x_i^* requires engineering judgment and is a way that physical understanding of the system being studied is incorporated in the analysis.

The input perturbation variables are scaled on the basis of their respective limits or authorities. Hence, define an $m \times m$ diagonal scaling matrix for input variables as

$$\mathbf{W}_u \equiv \text{diag}(u_1^*,\ u_2^*,\ \ldots,\ u_j^*,\ \ldots,\ u_m^*) \qquad (6)$$

where u_j^* is the maximum anticipated size for the input perturbation variable u_j. For controls, u_j^* are the control limits or authorities and are another example of how the physical characteristics of the system are included in the analysis. The largest possible magnitude of an input is then unity. A control input of ± 1 is then said to be against its stop (limit). Therefore, the scaling of the input variables is applied by letting

$$\mathbf{u} = \mathbf{W}_u \mathbf{u}^s \qquad (7)$$

Note that for many practical airplane problems, the control position limit is not symmetric about the trim control position. This point is further described later in the "Example Application" section.

Finally, the output perturbation variables are scaled by defining

$$\mathbf{y} = \mathbf{W}_y \mathbf{y}^s \qquad (8)$$

where $\mathbf{y}^s$ is a vector containing scaled output perturbation variables and $\mathbf{W}_y$ is a $l \times l$ diagonal matrix,

$$\mathbf{W}_y \equiv \text{diag}\,(y_1^*,\ y_2^*, \ldots,\ y_k^*,\ \ldots,\ y_l^*) \qquad (9)$$

where y_k^* is the maximum anticipated size for the output perturbation variable y_k. Like x_i^*, y_k^* should be chosen to define the region of linearity for the model.

Applying the scaling operations (eqs. (3), (7), and (8)) yields the system equations in scaled coordinates as

$$\left.\begin{aligned} \dot{\mathbf{x}}^s &= \mathbf{A}^s \mathbf{x}^s + \mathbf{B}^s \mathbf{u}^s \\ \mathbf{y}^s &= \mathbf{C}^s \mathbf{x}^s + \mathbf{D}^s \mathbf{u}^s \end{aligned}\right\} \qquad (10)$$

where the scaled system dynamics, input distribution, state-to-output distribution, and input-to-output distribution matrices are

$$\left.\begin{aligned} \mathbf{A}^s &= \mathbf{W}_x^{-1} \mathbf{A}\, \mathbf{W}_x \\ \mathbf{B}^s &= \mathbf{W}_x^{-1} \mathbf{B}\, \mathbf{W}_u \\ \mathbf{C}^s &= \mathbf{W}_y^{-1} \mathbf{C}\, \mathbf{W}_x \\ \mathbf{D}^s &= \mathbf{W}_y^{-1} \mathbf{D}\, \mathbf{W}_u \end{aligned}\right\} \qquad (11)$$

In subsequent developments, the superscript s denoting the scaled quantities is omitted for notational compactness.

Modal Analysis

It is often useful to evaluate airplane linearized dynamics in terms of the fundamental modes of motion. A system description in terms of its fundamental modes is often referred to as being in modal coordinates. In this section, the scaled system (eqs. (10)) is first transformed into modal coordinates. Then the controllability and observability matrices are manipulated to determine the relationships between the system modes, system inputs, and system outputs.

The following discussion assumes that the system dynamics matrix $\mathbf{A}$ has no repeated eigenvalues—a reasonable assumption for airplane dynamics. An eigenvalue defines a system's stability as well as natural frequency, damping ratio, and/or time constant of a given system mode. For each eigenvalue, there exists a corresponding eigenvector. Because eigenvectors define how the physical states participate in a given mode of motion, modes are often identified by examining the system eigenvectors (ref. 3).

Modal coordinates. Define the matrix $\mathbf{V}$ as a similarity transformation assembled from the eigenvectors of $\mathbf{A}$ as follows. For each real eigenvalue of $\mathbf{A}$, one column of $\mathbf{V}$ is set equal to the corresponding eigenvector. For each complex conjugate pair of eigenvalues of $\mathbf{A}$, one column of $\mathbf{V}$ is set equal to the real part of the corresponding eigenvectors, and the adjacent column is set equal to the imaginary part of either eigenvector (ref. 2). This definition of $\mathbf{V}$ results in a matrix composed entirely of real numbers.

A transformation between the scaled coordinates and the modal coordinates can be defined as

$$\left.\begin{aligned}\mathbf{x} &= \mathbf{V}\boldsymbol{\xi} \\ \boldsymbol{\xi} &= \mathbf{V}^{-1}\mathbf{x}\end{aligned}\right\} \tag{12}$$

Applying this transformation to the scaled system (eqs. (10)) yields an expression for the system in scaled modal coordinates:

$$\left.\begin{aligned}\dot{\boldsymbol{\xi}} &= \boldsymbol{\Lambda}\boldsymbol{\xi} + \boldsymbol{\Gamma}\mathbf{u} \\ \mathbf{y} &= \boldsymbol{\Phi}\boldsymbol{\xi} + \mathbf{D}\mathbf{u}\end{aligned}\right\} \tag{13}$$

where

$$\left.\begin{aligned}\boldsymbol{\Lambda} &= \mathbf{V}^{-1}\mathbf{A}\mathbf{V} \\ \boldsymbol{\Gamma} &= \mathbf{V}^{-1}\mathbf{B} \\ \boldsymbol{\Phi} &= \mathbf{C}\mathbf{V}\end{aligned}\right\} \tag{14}$$

Since the matrix $\mathbf{D}$ contains no information about the system states $\mathbf{x}$, the transformation to modal coordinates does not operate on $\mathbf{D}$, the input-to-output distribution matrix.

The matrices $\boldsymbol{\Lambda}$, $\boldsymbol{\Gamma}$, and $\boldsymbol{\Phi}$ can be used to gain physical insight into the system under consideration. The modal dynamics matrix $\boldsymbol{\Lambda}$ is in a block-diagonal form known as modified Jordan canonical form (ref. 4), each block containing the eigenvalue(s) of a system mode. First-order modes produce a single element on the diagonal equal to the real eigenvalue for that mode λ_i. As a result of the definition of $\mathbf{V}$, second-order modes are represented by 2×2 blocks with the real, σ_i, and imaginary, ω_i, parts of the complex conjugate eigenvalues on cross diagonals as in the following example:

$$\boldsymbol{\Lambda} = \begin{bmatrix} \lambda_1 & 0 & 0 & \cdots & 0 \\ 0 & \sigma_2 & \omega_2 & \cdots & 0 \\ 0 & -\omega_2 & \sigma_2 & \cdots & 0 \\ \vdots & \vdots & \vdots & \ddots & \vdots \\ 0 & 0 & 0 & \cdots & \lambda_n \end{bmatrix} \tag{15}$$

The modal controllability matrix $\boldsymbol{\Gamma}$ gives the degree to which each control variable can excite each mode:

$$\boldsymbol{\Gamma} = \begin{bmatrix} \gamma_{11} & \gamma_{12} & \cdots & \gamma_{1m} \\ \gamma_{21} & \gamma_{22} & \cdots & \gamma_{2m} \\ \gamma_{31} & \gamma_{32} & \cdots & \gamma_{3m} \\ \vdots & \vdots & \ddots & \vdots \\ \gamma_{n1} & \gamma_{n2} & \cdots & \gamma_{nm} \end{bmatrix} \tag{16}$$

A row of zero elements in $\boldsymbol{\Gamma}$ corresponding to a first-order mode or two rows of zero elements in $\boldsymbol{\Gamma}$ corresponding to a second-order mode indicate the uncontrollability of that mode.

The modal observability matrix $\boldsymbol{\Phi}$ gives the degree to which each mode is observed in each output variable:

$$\boldsymbol{\Phi} = \begin{bmatrix} \varphi_{11} & \varphi_{12} & \cdots & \varphi_{1n} \\ \varphi_{21} & \varphi_{22} & \cdots & \varphi_{2n} \\ \varphi_{31} & \varphi_{32} & \cdots & \varphi_{3n} \\ \vdots & \vdots & \ddots & \vdots \\ \varphi_{l1} & \varphi_{l2} & \cdots & \varphi_{ln} \end{bmatrix} \tag{17}$$

A column of zero elements in $\boldsymbol{\Phi}$ corresponding to a first-order mode or two columns of zero elements in $\boldsymbol{\Phi}$ corresponding to a second-order mode indicate the unobservability of that mode.

Engineers may examine $\boldsymbol{\Lambda}$, $\boldsymbol{\Gamma}$, and $\boldsymbol{\Phi}$ for relative types of comparisons as well as absolute measures of influence; that is, they usually compare rows or columns of numbers with each other—a burdensome process as the size of systems under consideration becomes large. This report proposes to precompute the numbers of interest and then organize them in an easily interpreted fashion.

Relative control effectiveness. Assuming that the terms in equations (13) have been scaled, some physical insight may be gained from comparing the terms of matrix $\boldsymbol{\Gamma}$. Engineers who use the modal controllability matrix $\boldsymbol{\Gamma}$ during airplane dynamics analysis typically gain the most insight from comparing the elements in a given row with each other. This is nontrivial for systems with complex modal pairs.

To simplify this process, Lallman's relative modal control effectiveness matrix (ref. 5) can be computed:

$$\mathbf{C}_e = \left[c_{e_{\ell,j}}\right] \tag{18}$$

For each nonzero row i in $\boldsymbol{\Gamma}$ that corresponds to a first-order mode ℓ in $\boldsymbol{\Lambda}$,

$$c_{e_{\ell,j}} = \frac{|\gamma_{i,j}|}{\sqrt{\sum_{j=1}^{m} \gamma_{i,j}^2}} \tag{19a}$$

where $\gamma_{i,j}$ is the element in the ith row and jth column in the matrix $\boldsymbol{\Gamma}$. If i corresponds to the first row in $\boldsymbol{\Gamma}$ for a controllable second-order mode ℓ in $\boldsymbol{\Lambda}$,

$$c_{e_{\ell,j}} = \frac{\sqrt{\gamma_{i,j}^2 + \gamma_{i+1,j}^2}}{\sqrt{\sum_{j=1}^{m} \left(\gamma_{i,j}^2 + \gamma_{i+1,j}^2\right)}} \tag{19b}$$

The ranges of the subscripts are

$$\left.\begin{aligned} i &= 1,\ 2,\ \ldots,\ n \\ j &= 1,\ 2,\ \ldots,\ m \\ \ell &= 1,\ 2,\ \ldots,\ n' \end{aligned}\right\} \tag{20}$$

where n is the number of system states and eigenvalues, m is the number of system inputs, and n' is the number of system modes. If the system under study has one or more second-order modes, n' is less than n. If the system has an uncontrollable mode, the corresponding row in $\mathbf{C}_e$ is defined to be the null vector. The elements in $\mathbf{C}_e$ are the normalized relative modal control factors. The dimension of $\mathbf{C}_e$ is $n' \times m$, and all elements in $\mathbf{C}_e$ are nonnegative and less than or equal to one.

The relative control effectiveness matrix $\mathbf{C}_e$ is used by individually looking at the matrix elements in each row (corresponding to a mode ℓ). A large value of $c_{e_{\ell,j}}$ indicates that the jth control perturbation has significant influence on the ℓth mode relative to the other control perturbations. A small value indicates a control perturbation that has little influence over that particular mode. Matrix elements in different rows of $\mathbf{C}_e$ cannot be compared since each row has been normalized individually. Applications of the relative control effectiveness matrix $\mathbf{C}_e$ include aiding the engineer in determining the best set of control effectors for a given system.

Relative output significance. The relative output significance matrix $\mathbf{O}$ is analogous to the relative control effectiveness matrix defined in the previous section. This matrix can be used to determine how much a particular mode can be observed in the various outputs of the physical system under study. Therefore, the relative output significance matrix $\mathbf{O}$ is defined as a matrix formed by the columns of $\mathbf{\Phi}$ normalized for each mode ℓ in $\mathbf{\Lambda}$:

$$\mathbf{O} = [o_{k,\ell}] \tag{21}$$

For each nonzero column i in $\mathbf{\Phi}$ that corresponds to a first-order mode ℓ in $\mathbf{\Lambda}$,

$$o_{k,\ell} = \frac{|\varphi_{k,i}|}{\sqrt{\sum_{k=1}^{l} \varphi_{k,i}^2}} \tag{22a}$$

where $\varphi_{k,i}$ is the element in the kth row and ith column of the matrix $\mathbf{\Phi}$. If i corresponds to the first column for an observable second-order mode ℓ in $\mathbf{\Lambda}$,

$$o_{k,\ell} = \frac{\sqrt{\varphi_{k,i}^2 + \varphi_{k,i+1}^2}}{\sqrt{\sum_{k=1}^{l} \left(\varphi_{k,i}^2 + \varphi_{k,i+1}^2\right)}} \tag{22b}$$

The ranges of the subscripts are

$$\left.\begin{aligned} i &= 1,\ 2,\ \ldots,\ n \\ k &= 1,\ 2,\ \ldots,\ l \\ \ell &= 1,\ 2,\ \ldots,\ n' \end{aligned}\right\} \tag{23}$$

where l is the number of system outputs. If the system under study has an unobservable mode, the corresponding column in $\mathbf{O}$ is defined to be the null vector. The elements in $\mathbf{O}$ are the normalized relative modal observability factors. The dimension of $\mathbf{O}$ is $l \times n'$, and all elements in $\mathbf{O}$ are nonnegative and less than or equal to one.

The relative output significance matrix $\mathbf{O}$ is used by individually looking at the matrix elements in each column (corresponding to a mode ℓ). A large value of $o_{k,\ell}$ indicates that the kth output strongly observes the ℓth mode relative to the other outputs of the system. Small values of $o_{k,\ell}$ indicate outputs that weakly observe a particular mode. Matrix elements in different columns of $\mathbf{O}$ cannot be compared since each column has been normalized individually. Applications of the relative output significance matrix $\mathbf{O}$ include aiding the controls engineer in determining which sensors best observe the system modes to be controlled.

Optimal Steady-State Response

The development in this section was motivated by a desire to provide an analysis and design technique analogous to the Lallman pseudo-control method (ref. 5). For airplane configurations with a large number of redundant control effectors, Lallman's method can be used to allow computation of feedback gains for a small number of pseudo controls (ref. 6). Lallman's method computes a controls blending vector to maximize and/or minimize the response of a set of system modes. It is conceptualized for control strategies that decouple certain modes. Several airplane dynamics and control problems, including longitudinal rigid-body motion, require a different control strategy. For this class of problems, a controls blending method is sought that would operate on the state perturbations of a system, rather than on the system modes.

Although there are many potential solutions to this challenge, the author chose to develop a method

based on the relationship between the system input perturbations and the steady-state response of the system as measured in the output perturbations. For this method to have validity, some proportional relationship must exist between the steady-state and the transient response of the physical states to the system inputs. Therefore, this method yields meaningful answers only for certain types of airplane dynamics and control problems.

The technique described in this section should be used with caution for airplanes with unstable modes. This is perhaps intuitive since any unstable mode (and at least one of its associated physical states), when excited by a system input, results in an infinite steady-state output perturbation response. It is also worth noting that the "steady-state" output response predicted by a linear model may lie outside the model's region of linearity (validity). The engineer must be aware of the above facts and use judgment.

The steady-state response of the system outputs due to a given set of system inputs can be determined as follows. The existence of a steady-state condition implies that

$$\dot{\mathbf{x}}_{ss} = \mathbf{0} \tag{24}$$

For aircraft, the steady-state condition typically restricts the model's reference condition to non-accelerating flight. Combining the steady-state condition (eq. (24)) with system equations (10) yields the steady-state scaled system equations

$$\mathbf{0} = \mathbf{A}\mathbf{x}_{ss} + \mathbf{B}\mathbf{u}_{ss} \tag{25a}$$

$$\mathbf{y}_{ss} = \mathbf{C}\mathbf{x}_{ss} + \mathbf{D}\mathbf{u}_{ss} \tag{25b}$$

where $\mathbf{A}$, $\mathbf{B}$, $\mathbf{C}$, and $\mathbf{D}$ are the scaled system dynamics, input distribution, state-to-output distribution, and input-to-output distribution matrices defined in equations (11).

The following development assumes that the system under study does not have any zero eigenvalues (singularities). When singularities exist, the system must be altered by deleting the physical state that causes $\mathbf{A}$ to be singular (heading angle ψ is a typical example).

Having stated this caveat, equation (25a) can be rewritten as

$$\mathbf{x}_{ss} = -\mathbf{A}^{-1}\mathbf{B}\mathbf{u}_{ss} \tag{26}$$

Substituting equation (26) into equation (25b) yields

$$\mathbf{y}_{ss} = \left(-\mathbf{C}\mathbf{A}^{-1}\mathbf{B} + \mathbf{D}\right)\mathbf{u}_{ss} \tag{27}$$

The values in the scaled steady-state output perturbation vector $\mathbf{y}_{ss}$ are directly related to the values in the scaled steady-state input perturbation vector $\mathbf{u}_{ss}$. Therefore, the matrix computed in equation (27) is an indication of the steady-state control power of each system input as measured in the system outputs. The goal is to determine the steady-state control distribution that maximizes a combination of selected outputs while minimizing a combination of undesired outputs.

The distribution matrix between the steady-state inputs and the steady-state outputs is defined as

$$\mathbf{Q} = -\mathbf{C}\mathbf{A}^{-1}\mathbf{B} + \mathbf{D} \tag{28}$$

Then let

$$\mathbf{u}_{ss} = \mathbf{c}\hat{u} \tag{29}$$

where $\mathbf{c}$ is a unit-length vector of relative input magnitudes and $\hat{u}$ is a scalar pseudo-control variable. Therefore, equation (27) becomes

$$\mathbf{y}_{ss} = \mathbf{Q}\mathbf{c}\hat{u} \tag{30}$$

Let $\mathbf{q}_k$ represent a column vector formed by the kth row of $\mathbf{Q}$. Form an objective function

$$J = \mathbf{c}^T \left(\sum_{\substack{\text{Outputs} \\ \text{to max.}}} \mathbf{q}_k \mathbf{q}_k^T - \sum_{\substack{\text{Outputs} \\ \text{to min.}}} \mathbf{q}_k \mathbf{q}_k^T + 10^{-5} \sum_{\substack{\text{Outputs} \\ \text{remaining}}} \mathbf{q}_k \mathbf{q}_k^T \right) \mathbf{c}\hat{u}^2 \tag{31a}$$

which is to be maximized irrespective of the value of $\hat{u}$ and subject to the constraint

$$\mathbf{c}^T\mathbf{c} = 1 \tag{31b}$$

The constraint in equation (31b) is chosen so that for the scaled system (eqs. (10)), the controls have maximum deflections of ± 1. The first term of J is a summation of the scaled steady-state output perturbations to be maximized by selection of $\mathbf{c}$, and the second term of J is a summation of the scaled steady-state outputs to be minimized by selection of $\mathbf{c}$. Outputs included in the remainder term of J have some nonoptimal value.

The implementation indicated by equations (31) was developed to allow selection of the minimum set of outputs to be optimized without causing numerical problems when using eigensystem decomposition software. However, this implementation is not without potential problems. The value chosen for

the remainder weighting (10^{-5}) is based on the author's experience with aircraft models using the scaling techniques described in this paper. This weighting must be sufficiently large to prevent numerical problems associated with the computer algorithm being used. Conversely, if the weighting is not sufficiently small relative to the elements in the row vectors $\mathbf{q}_k$, the "optimization" may correspond to one of the remainder outputs—an undesirable result. Proper scaling should prevent this problem, but the reader is advised nevertheless.

An equivalent formulation to equations (31) can be written as

$$\max\left(\frac{J}{\mathbf{c}^T\mathbf{c}}\right) = \max\left(\frac{\mathbf{c}^T\mathbf{S}\mathbf{c}}{\mathbf{c}^T\mathbf{c}}\right) \tag{32}$$

where

$$\mathbf{S} = \left(\sum_{\substack{\text{Outputs}\\ \text{to max.}}} \mathbf{q}_k\mathbf{q}_k^T - \sum_{\substack{\text{Outputs}\\ \text{to min.}}} \mathbf{q}_k\mathbf{q}_k^T + 10^{-5}\sum_{\substack{\text{Outputs}\\ \text{remaining}}} \mathbf{q}_k\mathbf{q}_k^T\right) \tag{33}$$

for which the solution is well-known (ref. 7) and described by

$$\max\left(\frac{\mathbf{c}^T\mathbf{S}\mathbf{c}}{\mathbf{c}^T\mathbf{c}}\right) = \lambda_{\max}(\mathbf{S}) \tag{34}$$

Therefore, the solution for $\mathbf{c}$ is the eigenvector which corresponds to $\lambda_{\max}(\mathbf{S})$, the maximum eigenvalue of the matrix $\mathbf{S}$.

In the development described in equations (30) through (34), it has been implicitly assumed that the steady-state system output perturbations to be maximized or minimized were of equal importance. If this is not satisfactory, the above development can be extended in a straightforward manner by applying different weights to distinguish between the steady-state outputs.

Display of Computed Functions

The previous section describes the computation of various vectors and matrices which the control system engineer can use to gain physical insight into the dynamic system under study. Graphic display of these quantities can further aid the engineer in quickly analyzing and understanding a dynamic system.

Therefore, a format was developed for graphically presenting the various vector and matrix quantities which are computed using the analysis techniques described previously. Both vectors and matrices are presented in a bar chart format as shown in figure 3. For matrices, multiple bar charts are plotted for the set of vectors that define a given matrix.

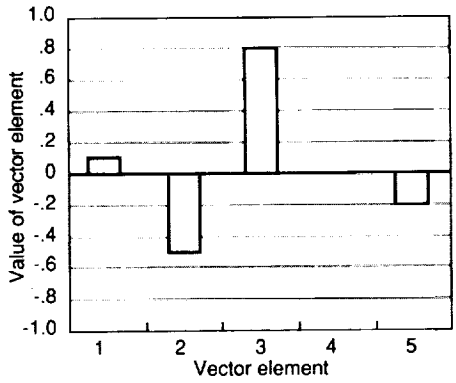

Figure 3. Bar chart format.

The bar chart vertical axis is the value of the vector elements. The horizontal axis indicates the elements of the vector. Each bar is located over an integer tick mark indicating a vector element. The height of the bar as measured against the vertical axis denotes the value of the vector element.

Example Application

In this section, an example application is described to illustrate some of the observations that can be made using the analysis techniques given in this report.

The example is a modern high performance airplane with a large number of redundant control effectors and hypothetical thrust vectoring in trimmed level flight at an angle of attack of 20°. Figure 4 is a drawing of the example high performance airplane. A thrust-vectoring system consisting of turning vanes configured as shown in figure 5 is postulated. For each engine, two turning vanes are used to deflect the exhaust flow. Each set of turning vanes is oriented so that each upper vane is rotated upward 48° from the airplane's horizontal axis. This thrust-vectoring system can generate control moments in the pitch, roll, and yaw axes. Note that yaw control moments cannot be generated without also generating roll control moments, and vice versa.

The analysis techniques were implemented using the MATRIX$_x$ software package. (MATRIX$_x$ is a registered trademark of Integrated Systems, Incorporated, Santa Clara, California.) The MATRIX$_x$ programming capability was used as the language for implementing the modal analysis techniques. Reference 8 lists some of the software used to analyze the examples.

The following linear system perturbation equations are for the example airplane at a trimmed, straight and level flight condition: altitude of 5000 ft, angle of attack of 20°, and total velocity of 235.1 ft/sec. The output perturbation variables are postulated by the author.

State-Space Description

The linear system perturbation equations for the example airplane are given in equations (2) where

$$\mathbf{x} = \{V_t \quad \alpha \quad q \quad \theta \quad \beta \quad p \quad r \quad \phi\}^T \tag{35a}$$

$$\mathbf{y} = \{V_t \quad \alpha \quad \beta \quad p \quad q \quad r \quad \phi \quad \theta\}^T \tag{35b}$$

$$\mathbf{u} = \left\{\delta_{s_{sy}} \quad \delta_{n_{sy}} \quad \delta_{f_{sy}} \quad \delta_{a_{sy}} \quad \delta_{tv_{sy}} \quad \delta_{th} \quad \delta_{s_{as}} \quad \delta_{f_{as}} \quad \delta_{a_{as}} \quad \delta_{tv_{as}} \quad \delta_r\right\}^T \tag{35c}$$

$$\mathbf{A} = \begin{bmatrix} -0.069 & -0.360 & 0 & -0.561 & 0 & 0 & 0 & 0 \\ -0.061 & -0.303 & 0.986 & 0 & 0 & 0 & 0 & 0 \\ -0.006 & -0.407 & -0.236 & 0 & 0 & 0 & 0 & 0 \\ 0 & 0 & 1.0 & 0 & 0 & 0 & 0 & 0 \\ 0 & 0 & 0 & 0 & -0.091 & 0.342 & -0.940 & 0.129 \\ 0 & 0 & 0 & 0 & -7.89 & -0.705 & 0.669 & 0 \\ 0 & 0 & 0 & 0 & -0.130 & 0.013 & -0.088 & 0 \\ 0 & 0 & 0 & 0 & 0 & 1.0 & 0.364 & 0 \end{bmatrix} \tag{35d}$$

$$\mathbf{B} = \begin{bmatrix} -0.120 & 0.104 & -0.095 & 0 & -0.026 & 0.168 & 0 & 0 & 0 & 0 & 0 \\ -0.070 & -0.006 & -0.047 & -0.025 & -0.016 & -0.015 & 0 & 0 & 0 & 0 & 0 \\ -1.69 & -0.091 & 0.145 & -0.133 & -0.529 & 0.028 & 0 & 0 & 0 & 0 & 0 \\ 0 & 0 & 0 & 0 & 0 & 0 & 0 & 0 & 0 & 0 & 0 \\ 0 & 0 & 0 & 0 & 0 & 0 & -0.003 & 0 & -0.002 & -0.015 & 0.014 \\ 0 & 0 & 0 & 0 & 0 & 0 & 2.95 & 3.48 & 2.52 & 0.223 & 0.382 \\ 0 & 0 & 0 & 0 & 0 & 0 & 0.005 & -0.061 & -0.095 & 0.420 & -0.290 \\ 0 & 0 & 0 & 0 & 0 & 0 & 0 & 0 & 0 & 0 & 0 \end{bmatrix} \tag{35e}$$

$$\mathbf{C} = \begin{bmatrix} 1 & 0 & 0 & 0 & 0 & 0 & 0 & 0 \\ 0 & 1 & 0 & 0 & 0 & 0 & 0 & 0 \\ 0 & 0 & 0 & 0 & 1 & 0 & 0 & 0 \\ 0 & 0 & 0 & 0 & 0 & 1 & 0 & 0 \\ 0 & 0 & 1 & 0 & 0 & 0 & 0 & 0 \\ 0 & 0 & 0 & 0 & 0 & 0 & 1 & 0 \\ 0 & 0 & 0 & 0 & 0 & 0 & 0 & 1 \\ 0 & 0 & 0 & 1 & 0 & 0 & 0 & 0 \end{bmatrix}$$

$$\mathbf{D} = \mathbf{O} \tag{35f}$$

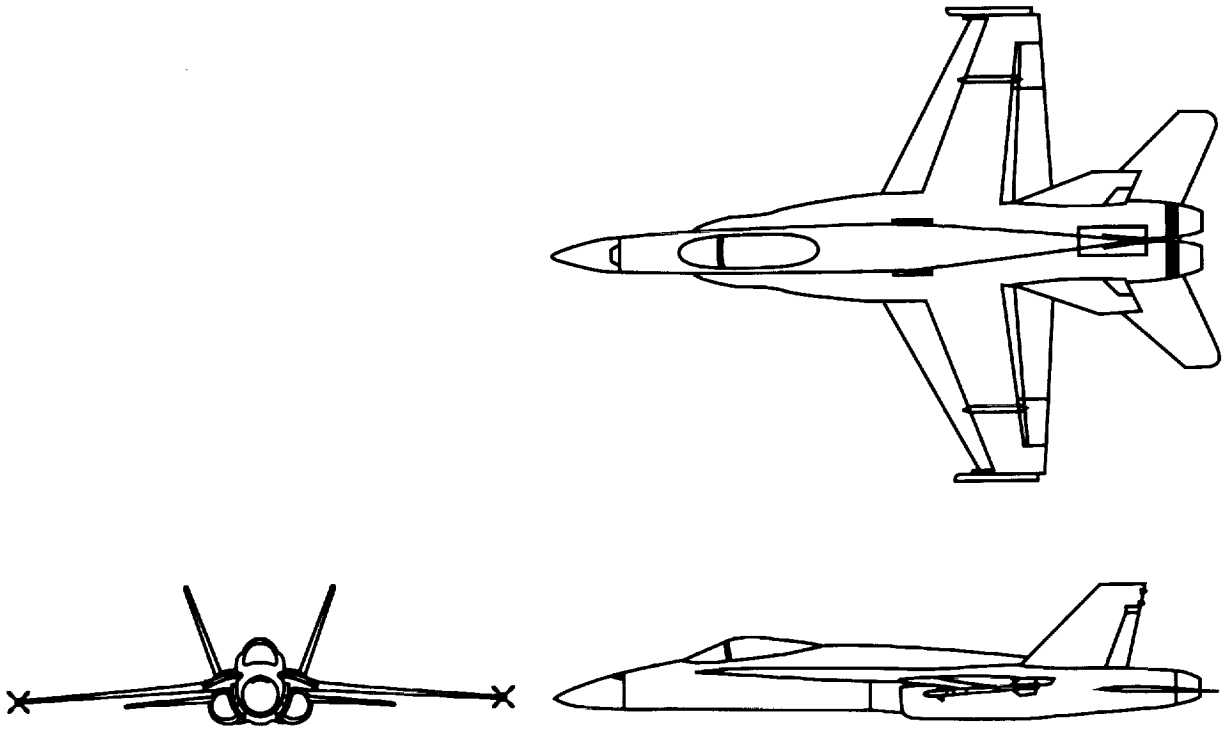

Figure 4. Example high performance airplane.

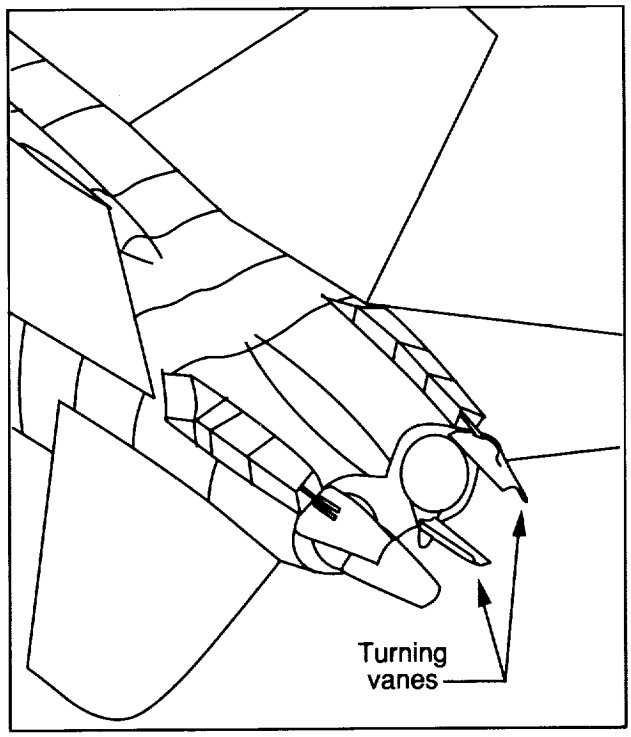

Figure 5. Postulated thrust-vectoring system.

All input perturbations (**u**) are in degrees. The total velocity (V_t) is in ft/sec; the velocity vector angles and Euler angles (α, β, ϕ, and θ) are in degrees; the body axis rates (p, q, and r) are in deg/sec.

Scaled Coordinates

The diagonal weighting matrices defined in equations (4), (6), and (9) must be determined to apply the scaling operations of equations (3), (7), and (8). The following guidelines are used to select the maximum expected values of the state perturbation variables used in equation (4):

1. Define V_t^* to be 10 percent of V_{t_0}, the total airplane velocity at trim.
2. Define α^* and β^* to maintain the airplane in the region of approximate linear aerodynamics about trim.
3. Define θ^* to be 5° and ϕ^* to be 10° (linear region for Euler angles about trim.)
4. Define p^* to equal ϕ^* in equivalent units (to maintain linearity in Euler angles for 1 sec).
5. Define q^* and r^* to equal one-fourth of p^*.

These guidelines result in

$$\begin{aligned}\mathbf{W}_x &= \text{diag}(V_t^*,\ \alpha^*,\ q^*,\ \theta^*,\ \beta^*,\ p^*,\ r^*,\ \phi^*) \\ &= \text{diag}(24,\ 5,\ 2.5,\ 5,\ 2.5,\ 10,\ 2.5,\ 10)\end{aligned} \tag{36}$$

These same guidelines are used to determine the maximum expected values of the output perturbation variables used in equation (9):

$$\begin{aligned}\mathbf{W}_y &= \text{diag}(V_t^*,\ \alpha^*,\ \beta^*,\ p^*,\ q^*,\ r^*,\ \phi^*,\ \theta^*) \\ &= \text{diag}(24,\ 5,\ 2.5,\ 10,\ 2.5,\ 2.5,\ 10,\ 5)\end{aligned} \tag{37}$$

Table 1 lists the guidelines used to select the maximum anticipated values of the input variables used in equation (6). Several issues associated with selection of the maximum anticipated size for airplane control input variables require engineering judgment. Each engineer may apply this judgment differently. During the analysis, the author developed two "rules" to describe how engineering judgment influenced the scaling methodology. The author offers these rules with the knowledge that they may be the subject of future debate.

Table 1. Guidelines for Scaling Input Variables

Variable	Description	Lower limit, deg	Upper limit, deg	Trim value, deg	Maximum anticipated size, deg
$\delta_{s_{sy}}$	Sym. horiz. stabilator	−24	10.5	−6.5	6.9
$\delta_{s_{as}}$	Antisym. horiz. stabilator	−10	10	0	10
$\delta_{n_{sy}}$	Sym. leading-edge flap	−3	34	26.6	7.4
$\delta_{f_{sy}}$	Sym. trailing-edge flap	−8	45	7.8	15.8
$\delta_{f_{as}}$	Antisym. trailing-edge flap	−8	8	0	8
$\delta_{a_{sy}}$	Sym. aileron	−25	42	0	1
$\delta_{a_{as}}$	Antisym. aileron	−25	25	0	24
$\delta_{tv_{sy}}$	Sym. thrust vectoring	−25	25	0	12.5
$\delta_{tv_{as}}$	Antisym. thrust vectoring	−25	25	0	12.5
δ_{th}	Throttle lever	31	106.5	89.6	16.9
δ_r	Rudder	−30	30	0	30

First, most of the symmetric and antisymmetric controls cannot be at their respective limits at the same time. As an example, antisymmetric thrust-vectoring vanes cannot be deflected when a full authority (25°), symmetric thrust-vectoring input is made. Therefore, the maximum anticipated values for these control effectors are reduced from the physical limits to allow simultaneous full authority deflections of the symmetric and antisymmetric controls. For some control effectors, such as the thrust-vectoring vanes, the maximum anticipated values allow equal authorities for the symmetric and antisymmetric controls. For other control effectors, such as the aileron, the maximum anticipated values favor one control (in this case, antisymmetric) over another.

Second, the most conservative maximum anticipated value is used for nonsymmetric control authorities about trim. An example of this rule, combined with the first rule, is the horizontal stabilator. The –6.5° trim position for symmetric horizontal stabilator $\delta_{s_{sy}}$ permits a deflection from trim of –17.5° and +16.9°. Applying the first rule reduces the permissible deflection to –7.5° and +6.9°. Therefore, the maximum anticipated value for $\delta_{s_{sy}}$ is 6.9°.

These guidelines for scaling the input variables result in

$$\begin{aligned}\mathbf{W}_u &= \mathrm{diag}(\delta^*_{s_{sy}},\ \delta^*_{n_{sy}},\ \delta^*_{f_{sy}},\ \delta^*_{a_{sy}},\ \delta^*_{tv_{sy}},\ \delta^*_{th},\ \delta^*_{s_{as}},\ \delta^*_{f_{as}},\ \delta^*_{a_{as}},\ \delta^*_{tv_{as}},\ \delta^*_r)\\ &= \mathrm{diag}(6.9,\ 7.4,\ 15.8,\ 1,\ 12.5,\ 16.9,\ 10,\ 8,\ 24,\ 12.5,\ 30)\end{aligned} \tag{38}$$

Modal Analysis

Modal coordinates. The system (eqs. (35)) is transformed into modal coordinates with the following result:

$$\mathbf{V} = \begin{bmatrix} 0 & -0.6543 & 0.0776 & 0 & 0.1599 & -0.1046 & 0 & 0 \\ 0 & 0.1573 & 0.0251 & 0 & 0.0803 & -0.6561 & 0 & 0 \\ 0 & -0.3048 & 0.1155 & 0 & 0.8983 & 0.0305 & 0 & 0 \\ 0 & 0.3692 & 0.8886 & 0 & -0.2764 & -0.6082 & 0 & 0 \\ -0.0705 & 0 & 0 & 0.0698 & 0 & 0 & 0.6268 & 0.3682 \\ 0.1675 & 0 & 0 & -0.2886 & 0 & 0 & -0.6451 & 0.5948 \\ -0.2774 & 0 & 0 & 0.1141 & 0 & 0 & -0.0055 & 0.0737 \\ -0.9434 & 0 & 0 & 0.9481 & 0 & 0 & 0.4370 & 0.3536 \end{bmatrix} \tag{39a}$$

$$\mathbf{\Lambda} = \begin{bmatrix} -0.1507 & 0 & 0 & 0 & 0 & 0 & 0 & 0 \\ 0 & -0.0053 & 0.1693 & 0 & 0 & 0 & 0 & 0 \\ 0 & -0.1693 & -0.0053 & 0 & 0 & 0 & 0 & 0 \\ 0 & 0 & 0 & -0.2934 & 0 & 0 & 0 & 0 \\ 0 & 0 & 0 & 0 & -0.2989 & 0.6026 & 0 & 0 \\ 0 & 0 & 0 & 0 & -0.6026 & -0.2989 & 0 & 0 \\ 0 & 0 & 0 & 0 & 0 & 0 & -0.2196 & 1.554 \\ 0 & 0 & 0 & 0 & 0 & 0 & -1.554 & -0.2196 \end{bmatrix} \tag{39b}$$

$$\mathbf{\Gamma} = \begin{bmatrix} 0 & 0 & 0 & 0 & 0 & 0 & 1.0968 & 2.400 & 8.333 & -13.30 & 22.72 \\ -1.324 & -0.1306 & 0.3395 & -0.0164 & -0.7594 & -0.1381 & 0 & 0 & 0 & 0 & 0 \\ -1.735 & -0.0917 & 0.4984 & -0.0158 & -1.001 & 0.1480 & 0 & 0 & 0 & 0 & 0 \\ 0 & 0 & 0 & 0 & 0 & 0 & 0.7685 & 2.054 & 7.538 & -13.02 & 22.03 \\ -5.378 & -0.3311 & 1.053 & -0.0625 & -3.056 & 0.1449 & 0 & 0 & 0 & 0 & 0 \\ -0.8951 & -0.0628 & 0.4556 & -0.0047 & -0.5342 & 0.0665 & 0 & 0 & 0 & 0 & 0 \\ 0 & 0 & 0 & 0 & 0 & 0 & -1.790 & -1.769 & -4.083 & 0.6504 & -2.002 \\ 0 & 0 & 0 & 0 & 0 & 0 & 3.078 & 3.081 & 7.070 & -1.395 & 4.046 \end{bmatrix} \tag{39c}$$

$$\Phi = \begin{bmatrix} 0 & -0.6543 & 0.0776 & 0 & 0.1599 & -0.1046 & 0 & 0 \\ 0 & 0.1573 & 0.0251 & 0 & 0.0803 & -0.6561 & 0 & 0 \\ -0.0705 & 0 & 0 & 0.0698 & 0 & 0 & 0.6268 & 0.3682 \\ 0.1675 & 0 & 0 & -0.2886 & 0 & 0 & -0.6451 & 0.5948 \\ 0 & -0.3048 & 0.1155 & 0 & 0.8983 & 0.0305 & 0 & 0 \\ -0.2774 & 0 & 0 & 0.1141 & 0 & 0 & -0.0055 & 0.0737 \\ -0.9434 & 0 & 0 & 0.9481 & 0 & 0 & 0.4370 & 0.3536 \\ 0 & 0.3692 & 0.8886 & 0 & -0.2764 & -0.6082 & 0 & 0 \end{bmatrix} \tag{39d}$$

The eigenvalues and eigenvectors of the system in equations (39) are listed in tables 2 and 3. All the system modes are stable. Note that the phugoid and short period modes are closer in natural frequency than is often the case for airplanes. The roll and spiral modes have similar characteristics because of the relatively high trim angle of attack.

Table 2. Eigenvalues of System

Eigenvalues	Natural frequency, sec^{-1}	Damping ratio, rad/sec	Time constant, sec	Period, sec	Time-to-half-amplitude, sec	Description
$\lambda_1 = -0.1507$			6.64		4.60	Spiral
$\lambda_2 = -0.0053 \pm i0.1693$	0.169	0.031		37.1	131	Phugoid
$\lambda_3 = -0.2934$			3.41		2.36	Roll
$\lambda_4 = -0.2989 \pm i0.6026$	0.673	0.444		9.34	2.32	Short period
$\lambda_5 = -0.2196 \pm i1.554$	1.57	0.140		4.00	3.16	Dutch roll

Table 3. Eigenvectors of System

State	Eigenvectors				
	Spiral	Phugoid	Roll	Short period	Dutch roll
V_t	0	$-0.65 \pm i0.08$	0	$0.16 \pm i0.10$	0
α	0	$0.16 \pm i0.03$	0	$0.08 \pm i0.66$	0
q	0	$-0.30 \pm i0.12$	0	$0.90 \pm i0.03$	0
θ	0	$0.37 \pm i0.89$	0	$-0.28 \pm i0.61$	0
β	-0.07	0	0.07	0	$0.63 \pm i0.37$
p	0.17	0	-0.29	0	$-0.65 \pm i0.59$
r	-0.28	0	0.11	0	$-0.01 \pm i0.07$
ϕ	-0.94	0	0.95	0	$0.44 \pm i0.35$

Relative control effectiveness. The relative control effectiveness matrix $\mathbf{C}_e$ defined in equations (19) is a collection of normalized relative modal control factors which enable comparison of the system inputs' effectiveness for a given mode:

$$\mathbf{C}_e = \begin{array}{c} \begin{matrix} \delta_{s_{sy}} & \delta_{n_{sy}} & \delta_{f_{sy}} & \delta_{a_{sy}} & \delta_{tv_{sy}} & \delta_{th} & \delta_{s_{as}} & \delta_{f_{as}} & \delta_{a_{as}} & \delta_{tv_{as}} & \delta_r \end{matrix} \\ \begin{bmatrix} 0 & 0 & 0 & 0 & 0 & 0 & 0.040 & 0.087 & 0.300 & 0.480 & 0.819 \\ 0.839 & 0.061 & 0.232 & 0.009 & 0.483 & 0.078 & 0 & 0 & 0 & 0 & 0 \\ 0 & 0 & 0 & 0 & 0 & 0 & 0.029 & 0.077 & 0.282 & 0.486 & 0.823 \\ 0.853 & 0.053 & 0.180 & 0.010 & 0.486 & 0.025 & 0 & 0 & 0 & 0 & 0 \\ 0 & 0 & 0 & 0 & 0 & 0 & 0.333 & 0.332 & 0.762 & 0.144 & 0.422 \end{bmatrix} \\ \begin{matrix} \text{Spir.} \\ \text{Phug.} \\ \text{Roll} \\ \text{S.P.} \\ \text{D.R.} \end{matrix} \end{array} \quad \begin{matrix} \\ \uparrow \\ \\ \downarrow \\ \\ \longleftrightarrow \end{matrix} \begin{matrix} \\ \text{Do not} \\ \\ \text{compare} \\ \\ \text{Compare} \end{matrix} \tag{40}$$

Figure 6 shows plots of the row vectors of $\mathbf{C}_e$ for the example airplane, the values for which are indicated in equation (40). The first six columns of matrix $\mathbf{C}_e$ correspond to the longitudinal (symmetric) inputs, while the remaining columns correspond to the lateral-directional (antisymmetric) inputs.

Recall that the rows of this matrix correspond to the system modes and the columns correspond to the system inputs. For example, the lower right element in $\mathbf{C}_e$ (0.422) indicates the effectiveness of the rudder on the Dutch roll mode relative to the other controls. Also recall that comparisons cannot be made between matrix elements in different rows of $\mathbf{C}_e$. For example, one cannot draw the conclusion that the rudder δ_r is more effective over the roll mode (0.823) than the Dutch roll mode (0.422).

Of all the controls, the symmetric stabilator $\delta_{s_{sy}}$ is the most effective in exciting both the phugoid and the short period mode; this is observed by comparing values in the second and fourth rows, respectively, of $\mathbf{C}_e$. The rudder δ_r is the most effective control in exciting the roll mode; this is observed by comparing values in the third row of $\mathbf{C}_e$. The rudder is less effective in exciting the Dutch roll mode than antisymmetric aileron $\delta_{a_{as}}$; this is seen by comparing values in the fifth row of $\mathbf{C}_e$.

Relative output significance. The relative output significance matrix $\mathbf{O}$ defined in equations (22) is a collection of normalized relative modal observability factors which enable comparison of the system outputs' ability to observe the motion of a given mode:

$$\mathbf{O} = \begin{array}{c} \begin{array}{ccccc} \text{Spir.} & \text{Phug.} & \text{Roll} & \text{S.P.} & \text{D.R.} \end{array} \\ \left[\begin{array}{ccccc} 0 & 0.540 & 0 & 0.145 & 0 \\ 0 & 0.130 & 0 & 0.503 & 0 \\ 0.071 & 0 & 0.070 & 0 & 0.571 \\ 0.168 & 0 & 0.289 & 0 & 0.689 \\ 0 & 0.267 & 0 & 0.684 & 0 \\ 0.277 & 0 & 0.114 & 0 & 0.058 \\ 0.943 & 0 & 0.948 & 0 & 0.442 \\ 0 & 0.788 & 0 & 0.508 & 0 \end{array}\right] \\ \longleftrightarrow \\ \text{Do not compare} \end{array} \begin{array}{l} V_t \\ \alpha \\ \beta \\ p \\ q \\ r \\ \phi \\ \theta \end{array} \quad \Big\updownarrow \text{Compare} \tag{41}$$

Figure 7 is a plot of $\mathbf{O}$ for the example airplane, the values for which are indicated in equation (41). The first, second, fifth, and eighth rows (vertical bars in fig. 7) correspond to the longitudinal outputs, while the remaining rows (vertical bars in fig. 7) correspond to the lateral-directional outputs.

Recall that the rows of this matrix correspond to the system outputs and the columns correspond to the system modes. For example, the third element in the rightmost column of $\mathbf{O}$ (0.571) indicates the appearance of the Dutch roll mode in the angle-of-sideslip output β relative to this mode's appearance in the other system outputs. Also recall that comparisons cannot be made between matrix elements in different columns of $\mathbf{O}$. For example, one cannot draw the conclusion that angle of attack α better observes the short period mode (0.503) than the phugoid mode (0.130).

The phugoid mode is primarily observed in θ and V_t; this can be seen by comparing values in the second column of $\mathbf{O}$. The short period mode is mostly observed in q, θ, and α; this is seen by comparing the elements of the fourth column of $\mathbf{O}$. Of all the outputs, the Euler roll angle ϕ best observes the roll mode; this is seen by comparing values in the third column of $\mathbf{O}$. The roll angle is less effective at observing the Dutch roll mode than both the roll rate p and the sideslip angle β; this is seen by comparing values in the fifth column of $\mathbf{O}$.

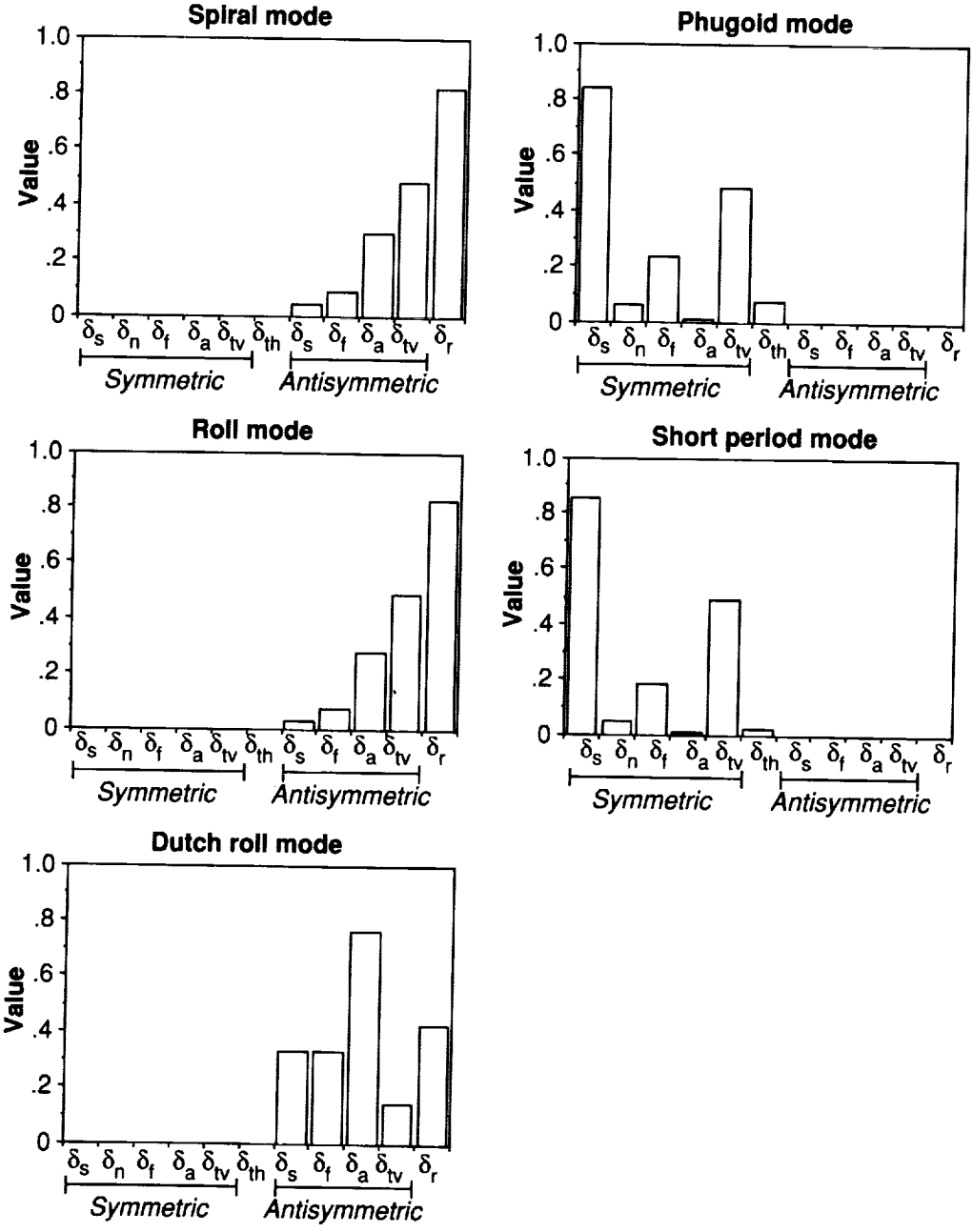

Figure 6. Relative control effectiveness matrix $\mathbf{C}_e$ for example airplane.

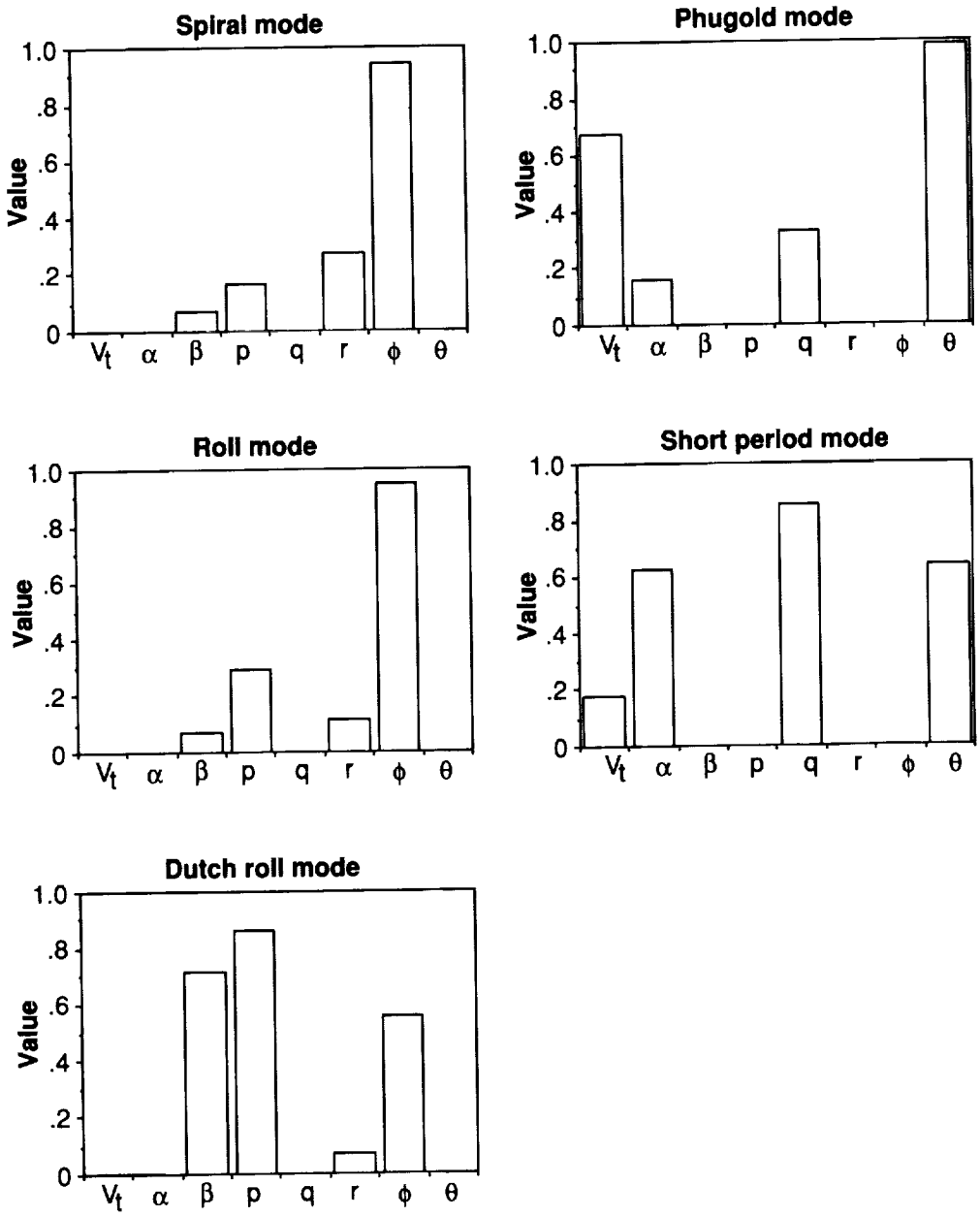

Figure 7. Relative output significance matrix **O** for example airplane.

Optimal Steady-State Response

The system's steady-state input-to-output distribution matrix **Q** is

$$\mathbf{Q} = \begin{array}{c} \begin{array}{ccccccccccc} \delta_{s_{sy}} & \delta_{n_{sy}} & \delta_{f_{sy}} & \delta_{a_{sy}} & \delta_{tv_{sy}} & \delta_{th} & \delta_{s_{as}} & \delta_{f_{as}} & \delta_{a_{as}} & \delta_{tv_{as}} & \delta_r \end{array} \\ \left[\begin{array}{ccccccccccc} 6.00 & 0.338 & -1.79 & 0.054 & 3.46 & -0.444 & 0 & 0 & 0 & 0 & 0 \\ -6.15 & -0.356 & 1.25 & -0.069 & -3.50 & 0.267 & 0 & 0 & 0 & 0 & 0 \\ 0 & 0 & 0 & 0 & 0 & 0 & 1.30 & 0.997 & 1.64 & 2.41 & -3.30 \\ 0 & 0 & 0 & 0 & 0 & 0 & 0.148 & 0.321 & 1.11 & -1.76 & 3.02 \\ 0 & 0 & 0 & 0 & 0 & 0 & 0 & 0 & 0 & 0 & 0 \\ 0 & 0 & 0 & 0 & 0 & 0 & -1.63 & -3.52 & -12.2 & 19.4 & -33.1 \\ 0 & 0 & 0 & 0 & 0 & 0 & -3.11 & -7.11 & -24.9 & 40.6 & -69.4 \\ 0.100 & 0.301 & -0.279 & 0.012 & 0.078 & 1.10 & 0 & 0 & 0 & 0 & 0 \end{array}\right] \end{array} \begin{array}{c} V_t \\ \alpha \\ \beta \\ p \\ q \\ r \\ \phi \\ \theta \end{array} \tag{42}$$

where the matrix **Q** is defined in equation (28). The rows in **Q** correspond to the system outputs and the columns correspond to the system control inputs. Note that the row in **Q** corresponding to the steady-state pitch rate perturbation output q_{ss} is a null vector. This is a direct result of the model structure and the imposition of the steady-state condition. Since the model was trimmed in straight and level flight, $\dot{\theta} = q$. Since $\dot{\theta}_{ss} = 0$, then $q_{ss} = 0$ for this model.

The blending of input perturbations to achieve an optimal steady-state response for a thrust-vectored fighter airplane can be computed as indicated in equations (30) through (34). Figure 8 plots the scaled (white bars) input control deflections that maximize response in the α_{ss} output perturbation, but do not minimize any steady-state outputs. The result is that the dominant controls are symmetric thrust vectoring and symmetric stabilator.

As discussed previously, when one desires to compute the relative sizes of input perturbations using these analysis techniques, proper scaling of the input variables is important. The shaded bars in figure 8 show the result of not applying the input scaling of equation (38) during the analysis. To arrive at this result, the blending vector **c** was computed for a version of the example system model with unscaled inputs. This **c** was then transformed to scaled coordinates and normalized to unit length for comparison purposes. Recall that the white bars indicate the values computed when the system inputs are scaled. Not scaling the inputs would cause inappropriate utilization of symmetric thrust vectoring, trailing-edge flaps, and aileron, resulting in suboptimal α_{ss} response.

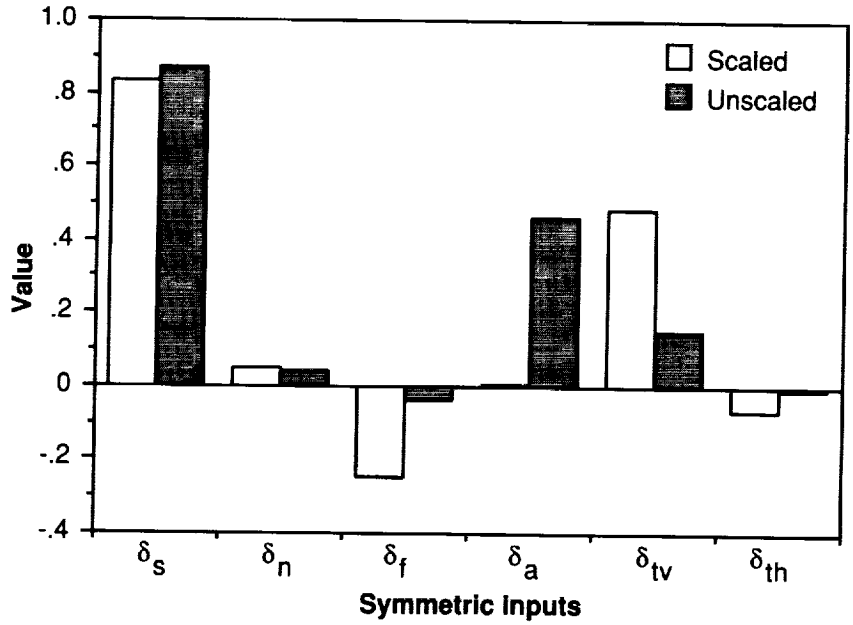

Figure 8. Input distribution that maximizes α_{ss} response (with and without input scaling).

Review

The most effective longitudinal control for the airplane model is the symmetric horizontal stabilator $\delta_{s_{sy}}$ as seen from the relative control effectiveness matrix $\mathbf{C}_e$. Similarly, examination of the relative control effectiveness matrix $\mathbf{C}_e$ indicates that the most effective lateral control is the rudder δ_r and the most effective directional control is antisymmetric aileron $\delta_{a_{as}}$.

With the exception of the spiral mode, the airplane modes are observed in their conventional outputs (e.g., the phugoid mode is observed in Euler pitch angle θ and total velocity V_t). The spiral mode was observed mostly in Euler bank angle ϕ since Euler heading angle ψ was not included in the model. The relative output significance matrix $\mathbf{O}$ indicates that all airplane modes are being observed; if control of the classical spiral mode is important, it may be necessary to add ψ as a system output to distinguish this airplane model's spiral mode from its roll mode for control design purposes.

The control deflections that optimized the α_{ss} response were consistent with the control effectiveness computations. For this example, input scaling affected the control deflection magnitudes for optimal α_{ss} response—especially for symmetric aileron $\delta_{a_{sy}}$ and symmetric thrust vectoring $\delta_{tv_{sy}}$.

Concluding Remarks

A systematic methodology has been outlined that transforms linear state-space matrix equations in physical coordinates to a set of matrix equations in scaled modal coordinates. The scaling processes are practical suggestions for handling the system units and control input limits that require an understanding of the system's physics. Guidelines for performing the scaling are indicated for the example airplane. Once the system was transformed to scaled modal coordinates, techniques were defined to analyze the effects of the system perturbation inputs on the fundamental modes of motion and the appearance of these modes in the system perturbation outputs. Also defined was a technique to compute a steady-state input perturbation vector that optimizes the steady-state response of selected output perturbations. Graphic formats were developed to display the vectors and matrices computed during the analysis. This was done to promote quick understanding of the analysis results for the dynamic system under study.

These analysis techniques have been applied to an example thrust-vectoring airplane model. This example is representative of the types of dynamics that are encountered in current vehicle designs. The results of this example application illustrate the understanding which can be acquired using the described modal analysis techniques.

The results of the analysis shown in this report can also be utilized directly in the control design process if desired. For example, the engineer can use the relative control effectiveness matrix to decide how the different control effectors should be allocated for various control tasks. Similarly, the relative output significance matrix can be used by the engineer to determine the appropriate set of sensors to use in observing the system modes. For many airplane control system designs, both these tasks can be easily accomplished using well-known heuristics instead of the approach described in this report. However, for many modern airplane designs, with a large number of control effectors (often redundant) and where active control of structural vibration modes must be accomplished simultaneously with control of the rigid-body modes, the relative control effectiveness and relative output significance analyses are of value. Finally, for the special case of an airplane configuration with a large number of redundant control effectors, the blending computation from the optimal steady-state response technique or the pseudo-control method of Lallman can be used to reduce the control law design by allowing computation of feedback gains for a small number of pseudo controls.

NASA Langley Research Center
Hampton, VA 23665-5225
February 6, 1991

References

1. Waszak, Martin R.; and Schmidt, David S.: *Analysis of Flexible Aircraft Longitudinal Dynamics and Handling Qualities. Volume I—Analysis Methods.* NASA CR-177943, Vol. I, 1985.
2. Strang, Gilbert: *Linear Algebra and Its Applications, Second ed.* Academic Press, Inc., c.1980.
3. Roskam, Jan: *Airplane Flight Dynamics and Automatic Flight Controls. Part I: Chapters 1 through 6—Rigid Airplane Flight Dynamics (Open Loop).* Roskam Aviation and Engineering Corp., c.1979.
4. Ogata, Katsuhiko: *State Space Analysis of Control Systems.* Prentice-Hall, Inc., c.1967.
5. Lallman, Frederick J.: *Relative Control Effectiveness Technique With Application to Airplane Control Coordination.* NASA TP-2416, 1985.
6. Lallman, Frederick J.: *Preliminary Design Study of a Lateral-Directional Control System Using Thrust Vectoring.* NASA TM-86425, 1985.
7. Wilkinson, J. H.: *The Algebraic Eigenvalue Problem.* Oxford Univ. Press, c.1965.
8. Arbuckle, P. Douglas: Modal Information Matrices for Analyzing Aerospace Vehicle Dynamics. M.S. Thesis, George Washington Univ., Dec. 1987.

NASA
National Aeronautics and Space Administration

Report Documentation Page

1. Report No.	2. Government Accession No.	3. Recipient's Catalog No.
NASA TP-3072		

4. Title and Subtitle	5. Report Date
A Controls Engineering Approach for Analyzing Airplane Input-Output Characteristics	April 1991
	6. Performing Organization Code

7. Author(s)	8. Performing Organization Report No.
P. Douglas Arbuckle	L-16798

9. Performing Organization Name and Address	10. Work Unit No.
NASA Langley Research Center Hampton, VA 23665-5225	505-66-71-03
	11. Contract or Grant No.

12. Sponsoring Agency Name and Address	13. Type of Report and Period Covered
National Aeronautics and Space Administration Washington, DC 20546-0001	Technical Paper
	14. Sponsoring Agency Code

15. Supplementary Notes

16. Abstract

An engineering approach for analyzing airplane control and output characteristics is presented. State-space matrix equations describing the linear perturbation dynamics are transformed from physical coordinates into scaled coordinates. The equations are scaled by applying various transformations that employ prior engineering knowledge of the airplane physics. Two analysis techniques are then explained. Modal analysis techniques calculate the influence of each system input on each fundamental mode of motion and the distribution of each mode among the system outputs. The optimal steady-state response technique computes the blending of steady-state control inputs that optimize the steady-state response of selected system outputs. An example airplane model is analyzed to demonstrate the described engineering approach.

17. Key Words (Suggested by Author(s))	18. Distribution Statement
Airplane dynamics Modal analysis Controls engineering Linear analysis	Unclassified—Unlimited Subject Category 08

19. Security Classif. (of this report)	20. Security Classif. (of this page)	21. No. of Pages	22. Price
Unclassified	Unclassified	20	A03

NASA FORM 1626 OCT 86

NASA-Langley, 1991

For sale by the National Technical Information Service, Springfield, Virginia 22161-2171